Chemical Engineering Journal 95 (2003) 47–55

Chemical Engineering Journal

www.elsevier.com/locate/cej

Cobalt catalysts for the oxidation of diesel soot particulate

Philip G. Harrison [a,1], Ian K. Ball [a], Wayne Daniell [b], Povilas Lukinskas [b,2], Matías Céspedes [c], Eduardo E. Miró [c], María A. Ulla [c,*]

[a] *School of Chemistry, University of Nottingham, University Park, Nottingham, NG7 2RD, UK*

[b] *Department Chemie, Physikalische Chemie, Ludwig Maximilians Universität, Butenandtstrasse 5-13, Haus E, D-81377 Munich, Germany*

[c] *Instituto de Investigaciones en Catálisis y Petroquímica, INCAPE (FIQ, UNL-CONICET), Santiago del Estero 2829, C.P. 3000 Santa Fe, Argentina*

Received 16 October 2002; accepted 3 March 2003

Abstract

Ceria-supported materials prepared by three routes, coprecipitation from aqueous solution containing both Co^{2+} and Ce^{3+} ions, and impregnation of preformed ceria gel with either cobalt(II) nitrate or cobalt(II) acetate, have been investigated for catalytic activity towards oxidation of diesel soot. All three materials catalyze the conversion of diesel soot particulate to carbon dioxide under a flow of either 6 vol.% O_2 or 0.5 vol.% NO + 6 vol.% O_2 in helium in the temperature range 573–613 K. The temperature of maximum conversion rate shows a small dependence on the particular catalyst and the composition of the oxidant. Raman spectroscopy of the ceria-supported cobalt catalysts indicate that the cobalt is present as Co_3O_4, but its average particle size in Co/CeO_2 impregnated with Co acetate is smaller than the other two Co/CeO_2 preparations. Features in the temperature-programmed reduction (TPR) profiles in the range 500–600 K, coincident with the temperature of catalytic activity, appear to be associated with reduction of the cobalt, suggesting a redox-type mechanism assisted by oxygen spillover on the CeO_2 support. In contrast, cobalt supported on alumina, silica, and tin(IV) oxide obtained by coprecipitation show much lower activity due to the presence of dispersed Co^{2+} ions in these materials although small amounts of Co_3O_4 may be present on alumina and tin(IV) oxide.

Keywords: Soot; Coprecepitation; Raman spectroscopy

1. Introduction

The deleterious effect on human health of particulate present in diesel emissions has become a subject of great concern, and has resulted in the formulation of restrictive legislation both in the EU and the US [1–5]. Such particulate matter is a complex multi-component material, comprising principally of carbonaceous soot particles but which also contain other smaller molecular compounds, many of which are toxic. Although physical filtration of the particulate from the exhaust emissions is possible, this solution has several drawbacks. The major problem is that a significant proportion of the particulate in the very small nano-range escape trapping, and it is particles in this dimension range that are considered to be the most dangerous diesel particulate fraction [5–7]. In addition, such physical traps suffer from blocking and need periodic regeneration. Further, other components of the exhaust emissions which are non-particulate in nature (HC's, CO, NO_x) will remain unaffected by physical filtration and, hence, be emitted unchanged into the atmosphere. However, the problem of particulate emissions is not only confined to diesel-powered vehicles. Even gasoline-powered automobiles equipped with three-way catalytic converters can emit particles similar than those emitted by diesel engines [8].

The alternative approach to the control of diesel emissions is similar to that adopted in the three-way catalytic converter for gasoline engines, i.e. the exhaustive catalytic conversion of the particulate to non-toxic CO_2 and H_2O. In general, since the solid particles are large, and when deposited immobile, they do not penetrate into the micro- and mesopore structure of the catalyst where catalytic processes usually take place. Rather, soot oxidation takes place on the wall of the matrix bed where the catalyst has been deposited, and hence the catalytic oxidation of soot is relatively slow. The situation is further complicated by the complex

* Corresponding author. Fax: +54-342-4536861.
E-mail addresses: p.g.harrison@nottingham.ac.uk (P.G. Harrison), mulla@fiqus.unl.edu.ar (M.A. Ulla).
[1] Co-corresponding author.
[2] Present address: Department of Organic Chemistry, Institute of Chemistry, A. Goštauto 9, LT 2600 Vilnius, Lithuania.

1385-8947/$ – see front matter © 2003 Elsevier Science B.V. All rights reserved.
doi:10.1016/S1385-8947(03)00077-9

chemical nature of diesel soot [9–13] and also the different size ranges of the particulate, and hence the catalytic oxidation processes are also complex in nature.

Various soot oxidation catalyst technologies have been developed. Indirect soot oxidation based on NO/NO_2 combustion with a temperature window of operation of 475–725 K has been commercialized by Johnson Matthey [14,15], but requires the use of low sulphur fuel [16]. Another way is to incorporate the catalyst during the soot-forming process by blending a stable organometallic additive into the fuel [17–21]. A large number of formulations have also been examined as catalysts for soot oxidation. Simple metal oxides (e.g. Co_3O_4, Cr_2O_3, CuO, Fe_2O_3, V_2O_5, MoO_3, and PbO) only operate satisfactorily at high temperatures (>775 K) [22], but a combination of metal oxide and an alkali impregnated on different supports notably improves their performance [20–24]. In this paper, we describe the activity of catalysts comprising ceria-supported cobalt towards the oxidation of diesel soot particulate, and compare these materials with similar catalysts supported in tin(IV) oxide, silica and alumina. We also analyse the effect of the support on the active species and soot oxidation mechanism.

2. Experimental

2.1. Catalyst preparation

2.1.1. Preparation of cobalt-promoted ceria by coprecipitation

Aqueous ammonia (AlanaR, 33 wt.%; 200 ml) was added dropwise to a solution of cerium(III) nitrate hexahydrate (Aldrich; 80 g; 0.184 mol) and cobalt(II) nitrate hexahydrate (Aldrich; 15 g; 0.0515 mol) in triply distilled water (TDW) (600 ml) in the presence of hydrogen peroxide (Aldrich; 20 volumes; 20 ml) over a period of 1 h to a final pH of 10. The mixture was then stirred overnight at ambient temperature and the resultant precipitate washed with triply distilled water and separated by centrifugation. The washing procedure was repeated four times and then the precipitate dried overnight in air at 333 K. The product took the form of a fine brown powder after manual grinding and is labeled as Co/CeO_2-cop.

2.1.2. Preparation of cobalt-promoted ceria by impregnation

2.1.2.1. Using cobalt(II) nitrate. Cobalt(II) nitrate hexahydrate (Aldrich; 47 g; 0.161 mol) was dissolved in TDW (200 ml) and the pH of the solution adjusted to 6.5 using dilute ammonia solution (0.2 M). CeO_2 (5 g) was then added and the mixture stirred for 16 h at ambient temperature after which the solid material was separated by filtration. After drying overnight in air at 333 K and grinding, the product took the form of a fine brown powder and is referred to as Co/CeO_2-imp/nit.

2.1.2.2. Using cobalt(II) acetate. The same procedure, as in Section 2.1.2.1, was adopted using cobalt(II) acetate tetrahydrate (Aldrich; 40 g; 0.137 mol). After drying overnight in air at 333 K and grinding, the product took the form of a fine brown powder and is referred to as Co/CeO_2-imp/acet.

2.1.3. Preparation of cobalt-promoted tin(IV) oxide by coprecipitation

Aqueous ammonia (AlanaR; 33 wt.%; 200 ml) was added dropwise to a solution of tin(IV) chloride (Aldrich; 75 g; 33 ml; 0.290 mol) and cobalt(II) nitrate hexahydrate (Aldrich; 17 g; 0.0584 mol) in triply distilled water (600 ml) over a period of 1 h to a final pH of 10. The mixture was then stirred overnight at ambient temperature and the resultant precipitate washed with triply distilled water and separated by centrifugation. The washing procedure was continued until the absence of chloride ions was confirmed by a negative result from the silver nitrate test, and the precipitate then dried overnight in air at 333 K. The product took the form of a fine grey powder after manual grinding and is referred to as Co/SnO_2-cop.

2.1.4. Preparation of cobalt-promoted alumina by coprecipitation

Aqueous ammonia (AlanaR; 33 wt.%; 200 ml) was added dropwise to a solution of auminium(III) nitrate nonahydrate (Aldrich; 75 g; 0.240 mol) and cobalt(II) nitrate hexahydrate (Aldrich; 3.2 g; 0.011 mol) in triply distilled water (600 ml) over a period of 1 h to a final pH of 10. The mixture was then stirred overnight at ambient temperature and the resultant precipitate washed with triply distilled water and separated by centrifugation. The washing procedure was repeated four times and the precipitate dried overnight in air at 333 K. The product took the form of a fine green powder after manual grinding and is referred to as Co/Al_2O_3-cop.

2.1.5. Preparation of cobalt-promoted silica by coprecipitation

Aqueous ammonia (AlanaR; 33 wt.%; 200 ml) was added dropwise to a solution of silicon(IV) chloride (Aldrich; 75 g; 50 ml; 0.446 mol) and cobalt(II) nitrate hexahydrate (Aldrich; 6.2 g; 0.0584 mol) in triply distilled water (600 ml) over a period of 1 h to a final pH of 10. The mixture was then stirred overnight at ambient temperature and the resultant precipitate washed with triply distilled water and separated by centrifugation. The washing procedure was continued until the absence of chloride ions was confirmed by a negative result from the silver nitrate test, and the precipitate then dried overnight in air at 333 K. The product took the form of a fine purple powder after manual grinding and is referred to as Co/SiO_2-cop.

2.1.6. Analytical and spectroscopic measurements

Prior to examination, each catalyst was calcined at 573 K overnight in a Vecstar91 tube furnace and then allowed to

cool to ambient temperature. Cobalt elemental analytical data were acquired using a wavelength dispersive Philips PW2400 X-ray fluorescence (XRF) spectrometer controlled by SuperQ software. The resultant data were then processed through the SemIQ semiquantitative software.

BET specific surface area measurements were carried out using Micromeritrics instrument. Crystalline phases of the catalyst materials were identified by powder X-ray diffraction using a Shimadzu XD-D1 diffractometer equipped with a Cu Kα ($\lambda = 1.5405$ Å) radiation source and using a scanning rate of 1°/min. The Shimadzu XD-D1 analysis software package was used for phase identification. Raman spectra were recorded under ambient conditions using a JASCO TRS-6000SZ-P Multichannel Laser Raman spectrometer. The excitation source was the 514.5 nm line of a Spectra 9000 Photometric Ar^+ laser, with laser power (measured at the sample) set at 31–40 mW.

2.2. Catalytic activity testing

Testing of the catalytic activity for diesel soot combustion was carried out on a fixed-bed flow system. The soot used in this work was prepared by burning commercial diesel fuel (Repsol-YPF, Argentina) in a glass vessel. After being collected from the vessel walls, it was dried on a stove at 393 K for 24 h [20]. The soot thus obtained, contained 70 ppm of sulfur. Its specific surface area was 55 m^2/g. Temperature-programmed experiments performed using helium as carrier gas provided information regarding the amount of partially oxidized groups of the soot surface and the amount of hydrocarbons that could remain adsorbed after the diesel combustion. In this way, the amount of carbon released as CO, CO_2 and hydrocarbons represents 9.3% of the soot [21]. Catalyst and soot (20:1 w/w) were carefully mixed, and approximately 10 mg of the mixture placed in an 8 mm quartz reactor. Two gas flow compositions were used: (i) 6 vol.% O_2; and (ii) 0.5 vol.% NO + 6 vol.% O_2, the balance being helium. The catalyst bed temperature was increased from 298 to 773 K at a rate of 8°/min with the feed gas flowing through the catalyst bed at a rate of 100 ml/min. The temperature of the catalyst bed was monitored by using a thermocouple. Analysis of the carbon dioxide evolved during the reaction was carried out by taking samples downstream every 30° which were stored in a 16-loop VALCO valve. After the reaction, the 16 samples were analyzed using a gas chromatograph containing a 5 Å zeolite column and TCD detector. The major product of the soot combustion is CO_2, only trace amounts of CO having been detected. This is due to the fact that Co-containing catalysts are also very active for the CO oxidation reaction [21]. All the samples were calcined for 4 h at 673 K prior to measurement.

2.3. Temperature-programmed reduction

Temperature-programmed reduction (TPR) measurements were carried out using a gas mixture of 5% H_2/95% N_2 (flow rates of 1.92 and 38.4 ml/min for H_2 and N_2, respectively). Parameters for the measurements (mass of reducible sample; gas flow rate; concentration of H_2) were optimized according to Monti and Baiker [25]. The samples (150 mg) were calcined at 673 K for 4 h, and then purged for 0.5 h at 298 K in N_2 before exposure to the reducing atmosphere, and simultaneously ramping of the temperature (5 K/min) up to 1200 K. H_2 consumption was measured using a thermal conductivity detector. CeO_2 and SnO_2 were run as reference materials under the same conditions.

3. Results

3.1. Diesel soot oxidation (O_2 and NO + O_2)

The catalytic activities for diesel soot particulate combustion over the three ceria-supported cobalt catalysts (Co/CeO_2-cop, Co/CeO_2-imp/nit, and Co/CeO_2-imp/acet) are compared by analyzing the CO_2 production/temperature profiles for oxidation using an 6 vol.% O_2/He mixture (Fig. 1) and a 0.5 vol.% NO/6 vol.% O_2/He mixture (Fig. 2). The CO_2 production maxima suggest that all three catalyst materials have similar activities with maxima in the temperature range 573–613 K. The maxima for the Co/CeO_2-cop and Co/CeO_2-imp/nit, catalysts are identical for both feed gas mixtures at 593 and 613 K, respectively. However, that for the Co/CeO_2-imp/acet material exhibits a distinct difference. The maximum is at a higher temperature (603 K) for the NO/O_2 mixture than for O_2 alone (573 K). No CO_2 is detected at temperatures in excess of 673 K for any of the catalysts with either feed gas indicating that all the soot has been combusted by this temperature. In contrast, the maximum soot combustion using unpromoted ceria occurs at a significantly higher temperature around 773 K [23]. Besides, in a previous work [21], blank experiments were performed mixing the soot with Al_2O_3 (a non-active solid

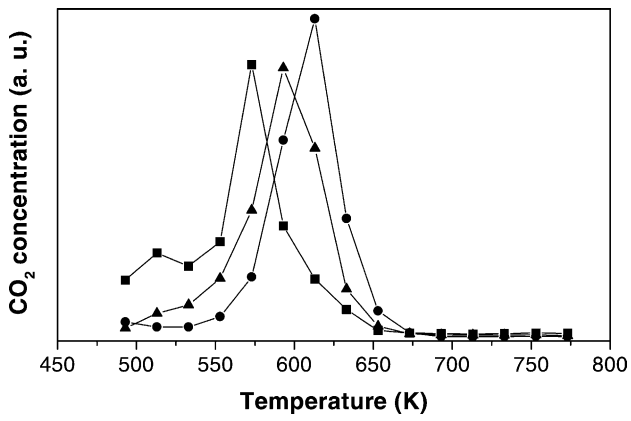

Fig. 1. TPO analysis of mechanical mixture of soot and the Co/CeO_2-cop (▲), Co/CeO_2-imp/nit (●), and Co/CeO_2-imp/acet (■) catalysts using an feed gas mixture of 6% O_2 in helium.

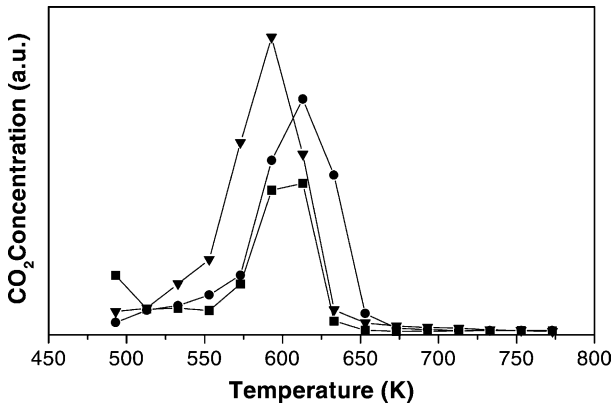

Fig. 2. TPO analysis of mechanical mixture of soot the Co/CeO_2-cop (▲), Co/CeO_2-imp/nit (●), and Co/CeO_2-imp/acet (■) catalysts using an feed gas mixture of 0.5% NO + 6% O_2 in helium.

for soot combustion) and the temperature-programmed oxidation profile had a maximum at ca. 873 K, and the soot was totally burnt at ca. 1023 K. The small feature present in the profiles for the Co/CeO_2-imp/acet for both feed gases at ca. 510 K may be possibly due to the decomposition of residual acetate.

The other three materials, Co/SiO_2-cop, Co/SnO_2-cop, and Co/Al_2O_3-cop, were distinctly less efficient (Fig. 3). Although the ignition temperatures for soot combustion were similar to the Co/CeO_2 catalysts (ca. 550 K), the carbon dioxide/temperature profiles (Fig. 3) for these materials are very broad with the maximum production being observed at temperatures of ca. 693 K for Co/SiO_2-cop and ca. 733 K for Co/SnO_2-cop and Co/Al_2O_3-cop. For all three of these materials, CO_2 remains downstream even at a bed temperature of 773 K showing that not all the soot is been combusted even at this temperature. It is worth noting that a small maximum is also present at 593 K, the same temperature as for the ceria-supported catalysts, for the Co/Al_2O_3-cop material.

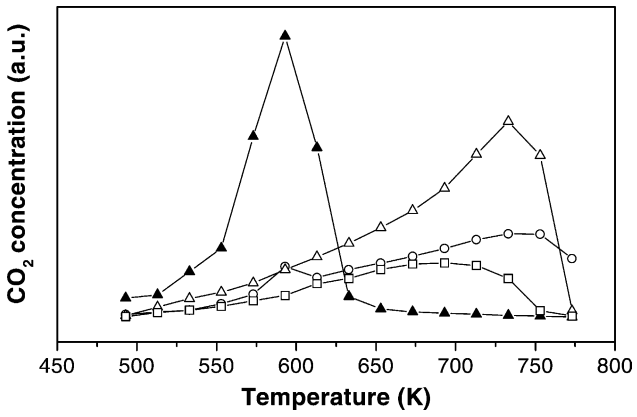

Fig. 3. TPO analysis of mechanical mixture of soot the Co/CeO_2-cop (▲), Co/SnO_2-cop (△), Co/Al_2O_3-cop (○) and Co/SiO_2-cop (□) catalysts using an feed gas mixture of 0.5% NO + 6% O_2 in helium.

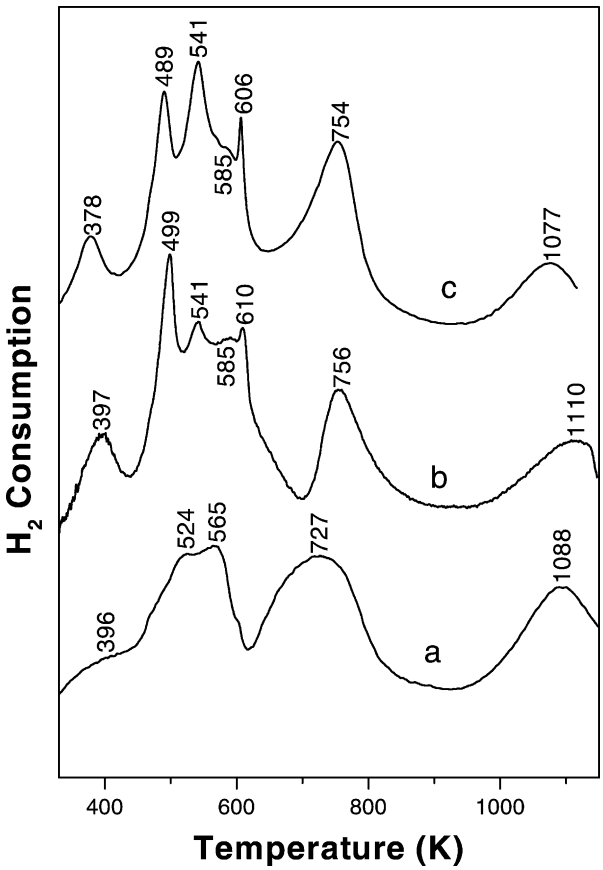

Fig. 4. TPR profiles for the Co/CeO_2-imp/acet (a), Co/CeO_2-cop (b), and Co/CeO_2-imp/nit (c) catalysts.

3.2. Temperature-programmed reduction

TPR profiles for the catalyst materials are shown in Figs. 4 and 5. The profiles for the three Co/CeO_2 materials are all very similar (Fig. 4). The feature observed in all three materials as well as in unpromoted ceria gel at ca. 380–400 K

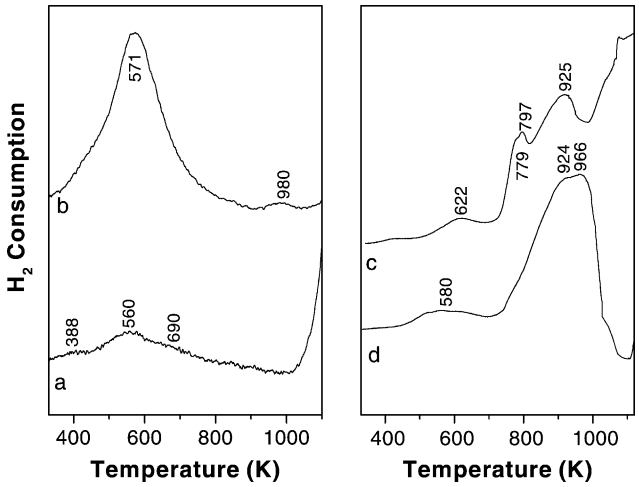

Fig. 5. TPR profiles for the Co/SiO_2-cop (a), Co/Al_2O_3-cop (b), Co/SnO_2-cop (c) catalysts, and SnO_2 (d).

is attributed to the reduction of surface hydroxyl groups (or other readily oxidized surface oxygen species) [26]. The features at 489, 541 and 585 K in Co/CeO_2-imp/nit (Fig. 4c), 499, 541 and 585 K in Co/CeO_2-cop (Fig. 4b), and 490 (shoulder), 524 and 565 K in Co/CeO_2-imp/acet (Fig. 4a) are attributed to reduction of the cobalt promoter within these materials whilst the sharp feature observed at ca. 610 K in the profiles of the Co/CeO_2-cop and Co/CeO_2-imp/nit materials are most likely due to residual nitrate ion. The remaining features in all three materials at 720–755 K can be attributed to the reduction of surface Ce^{4+} to Ce^{3+} in the ceria support, and at ca. 1110 K to bulk reduction of the ceria support.

Previous TPR studies have demonstrated that cobalt in different environments undergo reduction at different temperatures. For cobalt supported on alumina, four different temperature/reduction regimes have been observed: (i) Co_3O_4 crystallites undergo reduction at ca. 600 K; (ii) well-dispersed surface Co^{3+} ions at ca. 750 K; (iii) surface Co^{2+} ions at ca. 900 K; and (iv) subsurface Co^{2+} ions or phases such as $CoAl_2O_4$ which undergo reduction at ca. 1150 K [27,28]. The temperature at which reduction of cobalt occurs is strongly influenced not only by the oxidation state of the cobalt, but also by the nature of neighboring metal cations and/or metal oxide phases. The presence of neighboring Al^{3+} ions influences the reducibility of Co ions strongly, increasing the temperature for the reduction of Co^{2+} ions from ca. 900 to ca. 1150 K, which was rationalized by the polarization of Co–O bonds by the neighboring Al^{3+} ions [27].

In the present case, we attribute the features in the TPR profiles of the Co/CeO_2 catalyst materials in the temperature range 490–590 K to the presence of Co_3O_4 crystallites on the ceria support. The observation of different features in this temperature range would indicate an inhomogeneous distribution of Co_3O_4 crystallites on the ceria surface, suggesting that the average size of Co_3O_4 particles for Co/CeO_2-imp/acet be smaller.

The reducibility of the Co_3O_4 crystallites on ceria is somewhat enhanced compared to the reducibility of Co_3O_4 crystallites on alumina, and is probably associated with the presence of the redox-active ceria. A similar enhancement of reducibility has been observed in mixed Co_xO_y–CuO oxides which comprise spinels like $Co_{1-x}^{2+}Cu_x^{2+}[Co^{3+}]_2O_4$, Co_3O_4, and CuO after calcination at 723 K, the relative amount of each phase depending on the Co/Cu atom ratio. In these materials, TPR showed that the reduction is affected by a strong mutual influence between cobalt and copper. The reducibility of the mixed oxide catalysts was always promoted with respect to that of the pure Co_3O_4 and CuO phases and the reduction of cobalt was markedly enhanced by the presence of copper. Enhanced reducibility of cobalt was also observed when the mixed oxides were heated in nitrogen, when CoO, $CuCoO_2$ and CuO were formed [29]. In $CoO\text{-}MoO_3/Al_2O_3$ catalysts also, although the reduction of surface Mo^{6+} species is not affected by the presence of Co, the reduction of Co^{2+} ions is influenced strongly by the presence of Mo. The reduction maximum for dispersed Co^{2+} ions decreases from ca. 1200 K observed for CoO/Al_2O_3 to 800–850 K for $CoO\text{-}MoO_3/Al_2O_3$ [30].

The TPR profile for the Co/SiO_2-cop catalyst exhibits only a small broad feature at ca. 560 K, although there appears to be a much more intense feature at >1100 K which is attributable to dispersed Co^{2+} ions (Fig. 5a). The Co/Al_2O_3-cop catalyst shows a strong feature at ca. 570 K (Fig. 5b), which could arise from the reduction of Co_3O_4 crystallites. No reduction of the support oxide is apparent in either material although the Co/Al_2O_3 catalyst does show a very weak feature at 980 K which could also be due to reduction of a small amount of dispersed Co^{2+} ions. The profile for Co/SnO_2-cop (Fig. 5c) shows a weak feature at 622 K due reduction of a small amount of Co_3O_4 crystallites together with stronger features at 779 and 797 K attributable to the reduction of dispersed Co^{3+} ions [27,28]. The feature at 925 K is consistent with the reduction of the SnO_2 support (the feature at ca. 960 K in unpromoted SnO_2; Fig. 5d).

3.3. Raman spectroscopy

The Raman spectrum (Fig. 6c) of the Co/CeO_2-imp/nit catalyst material exhibits characteristic bands of Co_3O_4 at 669, 612, 498 and 459 cm^{-1} as well as a band at 440 cm^{-1} due to the ceria support. That of the Co/CeO_2-cop material is very similar (Fig. 6b), although the band of Co_3O_4 at 612 cm^{-1} is too weak to be observed. Surprisingly, that of the Co/CeO_2-imp/acet catalyst material is quite different,

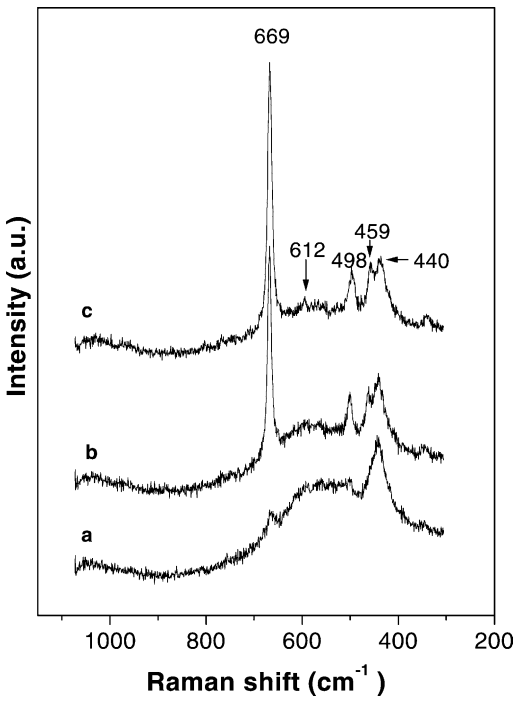

Fig. 6. Raman spectra for the Co/CeO_2-imp/acet (a), Co/CeO_2-cop (b) and Co/CeO_2-imp/nit (c) catalysts.

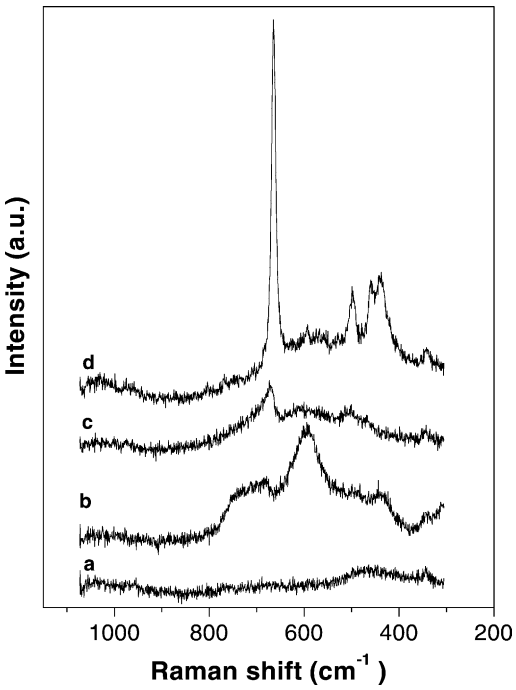

Fig. 7. Raman spectra for the Co/SiO_2-cop (a), Co/SnO_2-cop (b) and Co/Al_2O_3-cop (c) catalysts. The spectrum of Co/CeO_2-cop (d) is also shown for comparison.

exhibiting a broad band around 500 cm^{-1} and the band due to the ceria support at 440 cm^{-1} with the bands due to Co_3O_4 being much weaker (Fig. 6a). The broad band could be associated to small well-dispersed Co_3O_4 particles which are sustained by TPR profile of this material (Fig. 4a). Note that this kind of band is also observed in Co/CeO_2-cop spectrum (Fig. 6b).

Fig. 7 shows the Raman spectra of the Co/SiO_2-cop, Co/SnO_2-cop, and Co/Al_2O_3-cop materials. The former is completely featureless and devoid of any chemical information, whereas the latter does appear to exhibit weak bands due to Co_3O_4. The spectrum of Co/SnO_2-cop exhibits a series of broad overlapping bands in the region 750–450 cm^{-1} with maxima at ca. 680, 600 and 440 cm^{-1}. This envelope of bands is most probably due to the Sn–O lattice vibrations of the SnO_2 support, but the features at ca. 680 and 440 cm^{-1} may be due to the presence of Co_3O_4.

3.4. Powder X-ray diffraction

Powder X-ray diffractograms (not shown) for the three Co/CeO_2 catalyst materials show only peaks due to the ceria support. Line width analysis using the Scherrer equation indicated ceria crystallite sizes of <10 nm. No peaks due to either CoO or Co_3O_4 could be discerned, even though the amount of Co in the catalysts is between 7 and 16% (Table 1). Although, it is possible that any cobalt-containing phases may be masked by fluorescence effects due to the copper radiation source.

Table 1
Physical data for the catalyst materials

Catalyst material	Co loading (wt.%)	BET surface area (m^2/g)
Co/CeO_2-imp/acet	7.3	56
Co/CeO_2-imp/nit	8.1	54
Co/CeO_2-cop	7.6	57
Co/SiO_2-cop	5.8	241
Co/SnO_2-cop	16.1	122
Co/Al_2O_3-cop	14.9	376

4. Discussion

4.1. Active site and cobalt species

Ceria-supported materials prepared by three routes, co-precipitation from aqueous solution containing both Co^{2+} and Ce^{3+} ions, and impregnation of preformed ceria gel with either cobalt(II) nitrate or cobalt(II) acetate catalyze the conversion of diesel soot particulate to carbon dioxide under a flow of either 6 vol.% O_2 or 0.5 vol.% NO + 6 vol.% O_2 in helium in the temperature range 573–613 K. There is a small dependence of the temperature of maximum conversion on the particular catalyst and the composition of the oxidant feed gas. The temperature maxima for the Co/CeO_2-cop and Co/CeO_2-imp/nit are the same for both gas mixtures (593 and 613 K, respectively). However, for the Co/CeO_2-imp/acet material the temperature is somewhat higher (603 K) for the NO/O_2/He mixture than for the O_2/He mixture (573 K). These observations suggest that, whereas both the Co/CeO_2-cop and Co/CeO_2-imp/nit catalyst materials are similar in nature and performance, the Co/CeO_2-imp/acet material is different. Raman spectroscopy of the ceria-supported cobalt catalysts indicate that the cobalt is present as Co_3O_4 in the Co/CeO_2-cop and Co/CeO_2-imp/nit catalyst materials, but the crystallite size is too small to be measured by powder X-ray diffraction. On the other hand, the nature of the Co/CeO_2-imp/acet catalyst material appears to be somewhat different. The Raman spectrum exhibits a broad band which could be attributed to well-dispersed Co_3O_4 particles and the TPR envelope of peaks in the range ca. 480–600 K is consistent with the small particle size of this compound. Features in the temperature-programmed reduction profiles in the range 500–600 K, coincident with the temperature of catalytic activity, appear to be associated with reduction of the cobalt species (i.e. particulate Co_3O_4) present in these cobalt-ceria containing catalysts as was reported by Miró and coworkers [20–24]. The Co/CeO_2-imp/acet catalyst is more active than the other two when O_2/He is the feed gas but has a similar activity when the feed is NO/O_2/He. The lower maximum temperature may be associated with a better dispersion of Co_3O_4 particulate (i.e. smaller particles) since the contact between carbon particles and redox-active sites would be enhanced. Even though, the maximum hydrogen consumption in the range 490–590 K is at lightly higher temperatures

due to small Co-spinel particles, an improvement in carbon-active site contact would be achieved.

In contrast, cobalt supported on alumina, silica, and tin(IV) oxide obtained by coprecipitation show much lower activity, with significantly lower rates of CO_2 production at higher temperatures (693–733 K). Whereas, the Raman spectrum of Co/SiO_2-cop gives no indication of the presence of Co_3O_4, it is possible that this phase is present in both Co/SnO_2-cop and Co/Al_2O_3-cop. Some corroboration for this conclusion also comes from the TPR profile for Co/Al_2O_3-cop, which exhibits a feature at ca. 570 K.

It appears from the present study that two factors are important for high catalytic activity: (i) cobalt needs to be present in the catalyst as Co_3O_4; and (ii) the support oxide needs to be redox active, i.e. easily reducible and reoxidizable by gaseous oxidants such as O_2 and NO_2. Hence, the Co/CeO_2 materials which fulfil these criteria are very active, but the Co/SnO_2 material, which appears to comprise largely Co^{3+} ions dispersed over a redox-active support gives quite good CO_2 production but not until ca. 733 K. On the two redox-inactive supports, alumina and silica, which also appear to contain dispersed Co^{2+} ions, the conversion is much lower with peak maxima at temperature of 693–733 K. It is notable that a small maximum is observed in the conversion profile of Co/Al_2O_3-cop at 593 K suggesting that some Co_3O_4 is present in this material. The increase in catalytic activity of the tin(IV) oxide-, alumina- and silica-supported materials at higher temperatures is probably associated with the conversion of dispersed $Co^{2+/3+}$ ions to Co_3O_4. Bulk CoO is known to transform into Co_3O_4 on heating in air at temperatures of 673–773 K, and on alumina CoO has been observed to be mainly converted to Co_3O_4 by 723 K [27,28]. Another factor which is probably important is the strength or otherwise of promoter–support interactions. When these are weak, as in the case of ceria, permitting the cobalt promoter to cluster and form Co_3O_4 microcrystallites. However, when they are strong the cobalt remains as dispersed Co^{2+} ions and aggregation to form Co_3O_4 microcrystallites only occurs at more elevated temperatures.

4.2. Catalytic oxidation mechanism

The mechanistic nature of the oxidation of the soot particulate may involve either activation of carbon atoms within the particulate or the catalyst acting as a source of activated oxygen which can be regenerated. Some catalysts can oxidize soot particulate by catalyzing the formation of a mobile oxidant (e.g. NO_2), by providing redox sites for the oxidation [20,23,24] or by dissociating O_2 and transferring the resulting highly active O_{ads} to the soot particle in a spillover-type mechanism [31]. Mul et al. [32] demonstrated with labeled oxygen studies that oxygen spillover and redox oxidation can occur simultaneously. The dominating mechanism will depend on the degree of physical contact between the catalyst and the soot. Previous studies [22,33] have examined three types of physical contact between catalyst and soot particulate: (i) “loose contact” where mixing of soot and catalyst was performed just with a spatula; (ii) “tight contact” involving mixing with a mechanical mill; and (iii) “in situ contact” where diesel soot particulate was filtered from an exhaust stream on to a bed of catalyst particles. The activity of several metal oxides including Co_3O_4, Cr_2O_3, CuO, Fe_2O_3, V_2O_5, MoO_3 and PbO have been examined and compared with uncatalyzed conversion which has a maximum at >873 K [22,33]. “In situ contact” data are very similar to the “loose contact” results, temperature for maximum conversion rate Co_3O_4, Cr_2O_3, CuO, Fe_2O_3 and V_2O_5, all being in the range 823–873 K, only slightly better than non-catalytic soot combustion, with those for MoO_3 and PbO being somewhat lower at ca. 773–793 K. Some improvement was noted with “tight contact”, especially for Co_3O_4 which was lowered down to ca. 683 K and PbO to ca. 663 K. Miró et al. reported that for “tight contact”, supported Co, K catalysts burned the soot at temperatures lower than 675 K [20,23,24]. The fact that “tight contact” gave more efficient catalysis was attributed to a greater number of contact points between the soot particulate and catalyst particles, which are smaller and better dispersed.

For evaluation of intrinsic reaction mechanisms, physical phenomena like mass and heat transfer limitations must be minimized. Working under realistic soot–catalyst contact (loose contact) implies that physical phenomena become very important, thus decreasing the overall reaction rate. On the other hand, working under tight contact conditions is obviously not realistic but relevant in other to study the intrinsic catalytic chemistry, which is essential for a rational catalyst design.

In the present case, the catalytic conditions are essentially of the “tight contact” nature, and the temperatures at which maximum conversion occurs for the Co/CeO_2 catalysts (573–613 K) compare favorably with other oxide catalysts [20–24,33]. The widespread use of ceria-based materials as catalysts has been extensively reviewed [34], and the characteristics which are most relevant to their activity are the mobility of lattice oxygen ions, the high oxidizing power of Ce^{4+}, the $Ce^{3+/4+}$ redox couple, and the oxygen storage ability of the ceria lattice [34,35]. Surface oxygen deficiencies which are created during catalytic oxidation are readily regenerated via adsorption of molecular oxygen formation highly reactive surface superoxide (O_2^-) or peroxide (O_2^{2-}) species depending on the state of reduction of the ceria. Both superoxide and peroxide are intermediates in the general process of O_2 dissociation, leading to the incorporation of gas-phase oxygen as lattice oxygen [36–38]. Surface oxide vacancies can also be regenerated via the intermediate formation of surface nitrite and hyponitrite species by adsorption of NO [39]. However, Co/CeO_2 catalysts are more active than unpromoted CeO_2 [23]. Besides, the TPR profiles in the range 500–600 K associated with the reduction of Co oxide species, coincident with the temperature of catalytic activity suggesting a redox-type mechanism assisted by oxygen spillover on the CeO_2 sup-

port. Further work is in progress to elucidate the precise mechanism.

5. Conclusions

- Co/CeO_2 materials prepared by the three routes catalyze the conversion of diesel soot particulate to CO_2 and all the soot has been combusted by 673 K. The temperature of maximum conversion shows small dependence on the particular catalyst and the composition of the oxidant (573–613 K).
- For the above mentioned materials, features in the temperature-programmed reduction profiles in the range 500–600 K, coincident with the temperature of catalytic activity, appear to be associated with reduction of the Co_3O_4, suggesting a redox-type mechanism assisted by oxygen spillover on the CeO_2 support. The lower temperature of maximum soot conversion observed for Co/CeO_2-imp/acet may be associated with a better dispersion of Co_3O_4 (i.e. smaller particles).
- In contrast, cobalt supported on alumina, silica, and tin(IV) oxide obtained by coprecipitation show much lower activity due to the presence of dispersed Co^{2+} ions in these materials. This is due to the strong Co–support interaction the cobalt remains as dispersed Co^{2+} ions and aggregation to form Co_3O_4 microcrystallites only occurs at more elevated temperatures. Although small amounts of Co_3O_4 may be present on alumina and tin(IV) oxide.

Acknowledgements

The work carried out in Munich was funded by the Fonds der chemischen Industrie and Deutsche Forschungsgemeinschaft. MC, EEM and MAU wish to acknowledge to the financial support received from ANPCyT, CONICET and UNL (CAI + D'96). Thanks are also given to the Japan International Agency (JICA) for the donation of Raman and XRD equipment.

References

[1] T.G. Spiro, W.M. Stigliani, Chemistry of the Environment, Prentice-Hall, London, 1996.
[2] E. Mészáros, Fundamentals of Atmospheric Aerosol Chemistry, first ed., Akadémiai Kiadó, Budapest, 1999.
[3] Diesel-fuel exhaust is deemed less carcinogenic, Chem. Eng. (2000) 25.
[4] Diesel Emissions and Lung Cancer: Epidemiology and Quantitative Risk Assessment, Health Effects Institute, Cambridge (EU), 1999.
[5] A. Seaton, W. MacNee, K. Donaldson, D. Godden, Particulate air pollution and acute health effects, Lancet 345 (1995) 176.
[6] K. Donaldson, P.H. Beswick, P.S. Gilmour, Free radical activity associated with the surface of particles: a unifying factor in determining biological activity? Toxicol. Lett. 88 (1996) 293.
[7] J. Ferin, G. Oberdörster, D.P. Penney, Pulmonary retention of ultrafine and fine particles in rats, Am. J. Respir. Cell Mol. Biol. 6 (1992) 535.
[8] D.J. Rickeard, J.R. Bateman, Y.K. Kwon, J.J. McAughey, C.J. Dickens, Exhaust particulate size distribution: vehicle and fuel influences in light duty vehicles, SAE paper 961980, 1996.
[9] O.I. Smith, Fundamentals of soot formation in flames with application to diesel engine particulate emissions, Prog. Energy Combust. Sci. 7 (1981) 275.
[10] B.S. Haynes, H.G. Wagner, Soot formation, Prog. Energy Combust. Sci. 7 (1981) 229.
[11] D.B. Kittelson, Engines and nanoparticles: a review, J. Aerosol Sci. 29 (1998) 575.
[12] J.H. Johnson, S.T. Bagley, L.D. Gratz, D.G. Leddy, A review of diesel particulate control technology and emissions effects, SAE paper 940233, 1994.
[13] M. Lippmann, Environmental Toxicants: Human Exposures and Their Health Effects, Van Nostrand, New York, 1992.
[14] P. Hawker, N. Myers, G. Hüthwohl, H.Th. Vogel, B. Bates, L. Magnusson, P. Bronnenberg, Experience with a new particulate trap technology in Europe, SAE paper 970182, 1997.
[15] P. Hawker, G. Hüthwohl, J. Henn, W. Koch, H. Lüders, B. Lüers, P. Stommel, Effect of a continuously regenerating diesel particulate filter on non-regulated emissions and particle size distribution, SAE paper 980189, 1998.
[16] R. Allanson, B.J. Cooper, J.E. Thoss, A. Uusimäki, A.P. Walker, J.P. Warren, European experience of high mileage durability of continuously regenerating diesel particulate filter technology, SAE paper 2000-01-0480, 2000.
[17] G. Lepperhoff, H. Lüders, P. Barthe, J. Lemaire, Quasi-continuous particle trap regeneration by cerium-additives, SAE paper 950369, 1995.
[18] J. Lemaire, Eolys™ fuel-borne catalyst for diesel particulates abatement: a key component of an integrated system, Dieselnet Technical Report, 1999, Dieselnet diesel emissions online. http://www.dieselnet.com.
[19] P.J. Richards, M.W. Vincent, S.L. Cook, Operating experience of diesel vehicles equipped with particulate filters and using fuel additive for regeneration, SAE paper 2000-01-0474, 2000.
[20] CA. Querini, L.M. Cornaglia, M.A. Ulla, E.E. Miró, Catalytic combustion of diesel soot on Co, K/MgO catalysts. Effect of the potassium loading on activity and stability, Appl. Catal. B 20 (1999) 165.
[21] CA. Querini, M.A. Ulla, F. Requejo, J. Soria, U. Sedrán, E.E. Miró, Catalytic combustion of diesel soot particles, activity and characterization of Co/MgO and Co, K/MgO catalysts, Appl. Catal. B: Environ. 15 (1998) 5.
[22] J.P.A. Neeft, O.P. van Pruissen, M. Makklee, J.A. Moulijn, Catalysts for the oxidation of soot from diesel exhaust gases. II. Contact between soot and catalyst under practical conditions, Appl. Catal. B 12 (1997) 21.
[23] E.E. Miró, F. Ravelli, M.A. Ulla, L.M. Cornaglia, C.A. Querini, Catalytic combustion of diesel soot on Co, K supported catalysts, Catal. Today 53 (1999) 631.
[24] E.E. Miró, F. Ravelli, M.A. Ulla, L.M. Cornaglia, C.A. Querini, Catalytic diesel soot elimination on $Co\text{-}K/La_2O_3$ catalysts: reaction mechanism and the effect of NO addition, Stud. Surf. Sci. Catal. 130 (2000) 731.
[25] D.A.M. Monti, A. Baiker, Temperature-programmed reduction—parametric sensitivity and estimation of kinetic parameters, J. Catal. 83 (1983) 323.
[26] S. Bernal, G. Blanco, G. Cifredo, J.A. Perez-Omil, J.M. Pintado, J.M. Rodríguez-Izquierdo, Reducibility of ceria-lanthana mixed oxides under temperature-programmed hydrogen and inert gas flow conditions, J. Alloy Comp. 250 (1997) 449.
[27] P. Arnoldy, J.A. Moulijn, Temperature-programmed reduction of Co/Al_2O_3 catalysts, J. Catal. 93 (1985) 38.

[28] L. Ji, J. Lin, H.C. Zeng, Metal–support interactions in Co/Al_2O_3 catalysts: a comparative study on reactivity of support, J. Phys. Chem. B 104 (2000) 1783.
[29] G. Fierro, M.L. Jacono, M. Inversi, R. Gragone, P. Porta, TPR and XPS study of cobalt–copper mixed oxide catalysts: evidence of a strong Co–Cu interaction, Topics Catal. 10 (2000) 39.
[30] P. Arnoldy, M.C. Franken, B. Scheffer, J.A. Moulijn, Temperature-programmed reduction of $CoO\text{-}MoO_3/Al_2O_3$ catalysts, J. Catal. 96 (1985) 381.
[31] E. Baumgarten, A. Schuck, Oxygen spillover and its possible role in coke burning, Appl. Catal. 37 (1988) 247.
[32] G. Mul, F. Kapteijn, C. Doornkamp, J.A. Moulijn, Transition metal oxide catalyzed carbon black oxidation: a study with $^{18}O_2$, J. Catal. 179 (1998) 258.
[33] J.P.A. Neeft, M. Makkee, J.A. Moulijn, Metal oxides as catalysts for the oxidation of soot, Chem. Eng. J. 64 (1996) 295.
[34] A. Trovarelli, Catalytic properties of ceria and CeO_2-containing materials, Catal. Rev. Sci. Eng. 38 (1996) 439.
[35] S. Bernal, G. Blanco, M.A. Cauqui, G.A. Cifredo, J.M. Pintado, J.M. Rodriguez-Izquierdo, Influence of reduction treatment on the structural and redox behavior of ceria, Catal. Lett. 53 (1998) 51.
[36] A.S. Sass, V.A. Shvets, G.A. Savel'eva, N.M. Popova, V.B. Kazanskii, Mechanism of low-temperature oxidation of carbon monoxide on supported mixed catalysts containing noble metals and cerium oxide, Kinet. Katal. 27 (1986) 894.
[37] J. Soria, A. Martinez-Arias, J.C. Conesa, Spectroscopic study of oxygen adsorption as a method to study surface defects on CeO_2, J. Chem. Soc., Faraday Trans. 91 (1995) 1669.
[38] C. Li, K. Domen, K. Maruya, T. Onishi, Dioxygen adsorption on well-outgassed and partially reduced cerium oxide studied by FT-IR, J. Am. Chem. Soc. 111 (1989) 7683.
[39] A. Martinez-Arias, J. Soria, J.C. Conesa, X.L. Seoane, A. Arcoya, R. Cataluña, NO reaction at surface oxygen vacancies generated in cerium oxide, J. Chem. Soc., Faraday Trans. 91 (1995) 1679.